

# Biochemical Correlates of Temozolomide Sensitivity in Pediatric Solid Tumor Xenograft Models<sup>1</sup>

David S. Middlemas,<sup>2</sup> Clinton F. Stewart,  
Mark N Kirstein, Catherine Poquette,  
Henry S. Friedman, Peter J. Houghton, and  
Thomas P. Brent

Departments of Molecular Pharmacology [D. S. M., P. J. H., T. P. B.],  
Pharmaceutical Science [C. F. S., M. N. K.], and Biostatistics and  
Epidemiology [C. P.], St. Jude Children's Research Hospital,  
Memphis, Tennessee 38105, and Duke University Medical Center,  
Durham, North Carolina 27710 [H. S. F.]

## ABSTRACT

The antitumor activity of the methylating agent temozolomide has been evaluated against a panel of 17 xenografts derived from pediatric solid tumors. Temozolomide was administered p.o. daily for five consecutive days at a dose level of 66 mg/kg. Courses of treatment were repeated every 21 days for three cycles. Tumor lines were classified as having high, intermediate, or low sensitivity, determined by complete responses, partial responses, or stable disease, respectively. Overall, temozolomide induced complete responses in five lines and partial responses in three additional tumor lines, giving objective regressions in 47% of xenograft lines. Analysis of temozolomide plasma systemic exposure indicated that this dose level was relevant to exposure achieved in patients. Tumors were analyzed by immunoblotting for levels of *O*<sup>6</sup>-methylguanine-DNA methyltransferase (MGMT) and two mismatch repair proteins, MLH-1 and MSH-2. Tumors classified as having high or intermediate sensitivity had low or undetectable MGMT and expressed detectable MLH-1 and MSH-2 proteins. Tumors classified as having low sensitivity had either (a) high MGMT or (b) low or undetectable MGMT but were deficient in MLH-1. The relationship between p53 and response to temozolomide was also examined. *In vitro* temozolomide did not induce p21<sup>cip1</sup> in p53-competent NB-1643 neuroblastoma cells. Suppression of p53 function in NB1643 clones through stable expression of a trans dominant negative p53 (NB1643p53<sup>TDN</sup>) did not confer temozolomide resistance.

Similarly, tumor sensitivity to temozolomide did not segregate with p53 genotype or p53 functional status. These results indicate that MGMT is the primary mechanism for temozolomide resistance, but in the absence of MGMT, proficient mismatch repair determines sensitivity to this agent.

## INTRODUCTION

Temozolomide is a relatively novel anticancer methylating agent that has been approved in the United States for treatment of astrocytoma and is entering various phases of clinical evaluation against other tumors. Phase II trials in Europe have also confirmed some activity against melanoma (1) and suggest activity against high-grade gliomas (2). This drug in many ways resembles more established compounds, such as dacarbazine and procarbazine (3), in that it gives rise to a methyl diazonium ion that attacks nucleophilic sites including the *O*<sup>6</sup>-guanine position in DNA. Temozolomide, however, differs from these drugs, which have to be activated by enzymatic oxidation (3), in that it degrades spontaneously via base-catalyzed hydrolysis to the final active methylating species.

Temozolomide is believed to exert its toxic effects primarily by generating *O*<sup>6</sup>-methylguanine in DNA (4). This adduct is subject to a single-step, error-free repair reaction that simply transfers the methyl group to a cysteine residue within the repair protein MGMT,<sup>3</sup> thus restoring the DNA to its intact state. Hence, MGMT is a major determinant of temozolomide cytotoxicity (5, 6).

*O*<sup>6</sup>-Methylguanine in itself is not deleterious to cells and does not inhibit DNA enzymatic processes such as replication or transcription. However, the preferred base pairing during DNA synthesis results in incorporation of thymine opposite *O*<sup>6</sup>-methylguanine instead of cytosine that results in a G:C to G:T transition mutation if not repaired. The *O*<sup>6</sup>-methylG:T mismatch is recognized by the MMR pathway of the cell (7), which proceeds to excise the errant thymine residue in the daughter strand, however, unless the *O*<sup>6</sup>-methylG is repaired before the resynthesis step in MMR, thymine is likely to be reinserted opposite the lesion. It is believed that the ensuing repetitive cycle of futile MMR results in generation of a chronic strand break condition that elicits an apoptotic response (Fig. 1). Cells treated with methylating agents such as temozolomide have indeed been observed to die via apoptosis (8).

Intact MMR function is thus critically required for the cytotoxicity of the methylating drugs. Of five or more distinct

Received 10/7/99; revised 12/13/99; accepted 12/13/99.

The costs of publication of this article were defrayed in part by the payment of page charges. This article must therefore be hereby marked advertisement in accordance with 18 U.S.C. Section 1734 solely to indicate this fact.

<sup>1</sup> Supported in part by United States Public Health Service awards CA71628, CA23099, CA14799, and CA21765 (Cancer Center Support Grant) from the National Cancer Institute and by American, Lebanese, Syrian Associated Charities.

<sup>2</sup> To whom requests for reprints should be addressed, at Molecular Pharmacology, St. Jude Children's Research Hospital, 332 North Lauderdale Street, Memphis, TN 38105-2794. Phone: (901) 495-3440; Fax: (901) 521-1668; E-mail: david.middlemas@stjude.org.

<sup>3</sup> The abbreviations used are: MGMT, *O*<sup>6</sup>-methylguanine-DNA methyltransferase; CR, complete response; PR, partial response; MMR mismatch repair; TDN, trans-dominant negative; MCR, maintained complete response; MTD, maximum tolerated dose; AUC, area under the concentration-time curve; HRP, horseradish peroxidase.

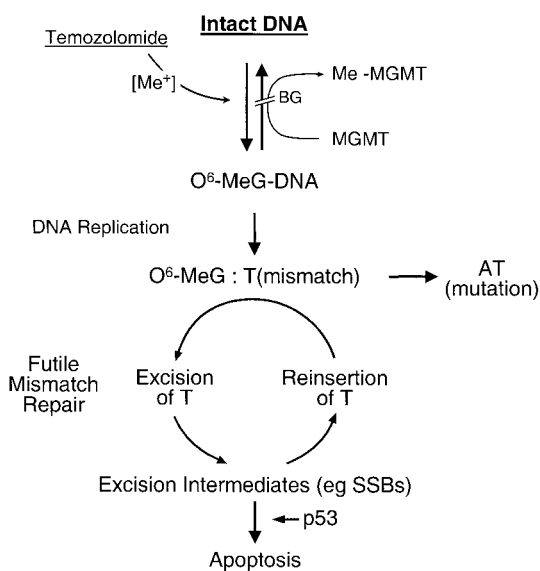


Fig. 1 Schematic of damage, repair, and apoptotic pathways potentially responsible for temozolomide cytotoxicity and resistance.

proteins that are involved in the MMR pathway (9), two, MLH-1 and MSH-2, have frequently been found to be suppressed in tumor cells (10). One would predict, based on current knowledge of these DNA repair pathways involved in the cytotoxic response to temozolomide, that for maximum sensitivity, tumors should lack MGMT and have high MMR activity (11). Tumors with high MGMT levels or lacking competent MMR function would be predicted to be drug resistant. The role of the p53 tumor suppressor gene in cellular sensitivity to temozolomide is less clear. Temozolomide can induce apoptosis in cells with or without functional p53 (12). However, Tentori *et al.* (8) reported that expression of p53 sensitized MGMT-proficient HL60 leukemia cells to temozolomide, although treatment did not induce G<sub>1</sub> arrest in these cells. D'Atri *et al.* (13) reported temozolomide induction of p53 in cells proficient in MMR but not in cells deficient in MMR. These results suggest signaling between MMR and p53-mediated apoptosis.

In the present study, we have tested these predictions by both determining the responses to temozolomide treatment of human solid tumor xenografts growing in mice and assessing the levels of MGMT and the MMR proteins MLH-1 and MSH-2 in these tumors. We have also related tumor sensitivity *in vitro* and *in vivo* to p53 genotype/phenotype. Our results indicate that MGMT and MMR repair functions do in fact correlate with *in vivo* response. However, the relationship between p53 status and temozolomide sensitivity is less clear.

## MATERIALS AND METHODS

**Tumor Models.** Each of the xenografts used has been described previously (14–16). Studies used six lines each of neuroblastoma and rhabdomyosarcoma, and four brain tumors. Rh28c tumors were established from a cell line derived from the Rh28 xenograft. Rh30c was established *in vitro* from the patient biopsy, maintained in culture for >1 year, and then established

as a xenograft. In contrast, Rh30 was established directly as a xenograft from the same biopsy material. Tumors were grown in the s.c. space of immune-deprived female CBA/CaJ mice, as described (14).

**Tumor Response and Tumor Failure Time.** For individual tumors, PR was defined as a volume regression > 50% but with measurable tumor ( $\geq 0.10 \text{ cm}^3$ ) at all times. CR was defined as a disappearance of measurable tumor mass ( $< 0.10 \text{ cm}^3$ ) at some point within 12 weeks after initiation of therapy. MCR was defined as CR without tumor regrowth within a 12-week study time frame. This time point was chosen because most studies lasted 12 weeks. Because tumors were implanted in both dorsal flanks of each mouse, a mouse is said to achieve a CR only if tumors on both flanks have CRs and a PR only if the tumor of at least one flank has a PR and the tumor response on the other flank is not worse than a PR. If an initial tumor volume was less than  $0.20 \text{ cm}^3$ , data on that tumor were excluded.

Tumor failure time was defined as the time (in weeks) required by individual tumors to quadruple their volume from the initiation of therapy. Tumor failure times were censored if a mouse died prior to week 12 and before a tumor grew to four times its initial volume. Because tumors were implanted in both lateral flanks, the tumor failure times from each mouse are clustered observations. Evidence of high correlation between failure times has been reported previously (17). Because the individual mouse is the unit of the experiment, the response of each mouse was taken to be the lesser of the two tumor failure times. This approach implicitly accounts for the clustering effect due to the mouse without explicitly specifying the correlation structure.

**Statistical Methods.** For comparisons of time to tumor failure for different treatment regimens, Kaplan-Meier estimates of failure distributions were obtained, and survival distributions of each treatment group were compared to the survival distribution of the control group using the exact log-rank test. Experiment-wise, significance level was maintained at 0.05 by using the Bonferroni procedure (18) to adjust for the multiplicity of tests of significance within each tumor line. SAS 6.12 and StatXact-4 were used for statistical analysis.

**Definition of Tumor Sensitivity.** Tumors have been classified as demonstrating high, intermediate, or low sensitivity based on the following response criteria. In the high sensitivity group, all tumors regressed completely (CR) with no tumor regrowths during the period of experimentation (mice were euthanized at week 12 after start of treatment); intermediate sensitivity indicated that all tumors demonstrated  $\geq 50\%$  regression (PR) but CRs were not maintained at week 12; and low sensitivity indicated that treatment groups had tumors that demonstrated <PR or progressive tumor growth during treatment. To estimate the response nadir (*i.e.*, maximum regression) and duration of regression (*i.e.*, tumor volume recovered to that at the start of treatment), mean relative tumor volumes for groups of tumors within a treatment group were calculated as relative tumor volume = volume at day *x* after treatment/volume at initiation of treatment over the 12 week period between starting treatment and terminating the experiments.

**Drug Formulation and Administration.** Temozolomide, generously provided by Schering-Plow Research Institute,

was dissolved in sterile water and administered by oral gavage. Efficacy was determined after administration for 5 consecutive days repeated every 21 days for three cycles. The highest daily dose tolerated for three cycles of therapy was 66 mg/kg on this schedule.

**Pharmacokinetics.** Following a single oral dose of temozolomide (66 mg/kg), blood samples were collected from mice (three animals per point) at 0, 0.25, 0.5, 1, 1.5, 2, 3, and 6 h. All samples were immediately centrifuged at 5.5 g for 2 min in a tabletop refrigerated centrifuge at 4°C. Serum was then divided into aliquots for processing to assay either temozolomide or MTIC. Temozolomide serum samples (800  $\mu$ l) were treated with 80 ml of 1.0 N HCl, and 100  $\mu$ l of this acidified plasma was further diluted with 400 ml of 0.1 N HCl. Ethazolastone was added as an internal standard prior to extraction with ethyl acetate. The organic phase was separated, isolated and dried under a stream of nitrogen. The dried pellet was resuspended in 800 ml of mobile phase, and 100  $\mu$ l were injected onto an isocratic high-performance liquid chromatograph using UV detection (19, 20). Plasma samples for MTIC (400  $\mu$ l) were treated with 800 ml of cold methanol, stored on ice for 5 min, vortexed, and centrifuged at 5.5  $\times$  g for 2 min. An aliquot (50  $\mu$ l) was combined with 60  $\mu$ l of mobile phase consisting of methanol:50 mM ammonium phosphate, pH 6.5 [20:80 (v/v)], and analyzed by high-performance liquid chromatography (21). These methods were determined to be precise (intraday and interday CV, 3.1 and 4.9% for temozolomide and 5.1 and 7.6% for MTIC, respectively) at temozolomide concentrations ranging from 50 to 1000 mg/ml and MTIC concentrations ranging from 0.2 mg/ml to 6 mg/ml

Temozolomide and MTIC plasma concentration-time data were analyzed using noncompartmental methods. The apparent time of maximum concentration ( $t_{max}$ ) and maximum plasma concentration ( $C_{max}$ ) were noted. The AUC for temozolomide and MTIC was calculated using the logarithmic trapezoidal method (22). The terminal elimination rate constant ( $\beta$ ) was determined by log-linear least-squares regression of the plasma concentration time points in the terminal phase of the plasma disposition curve. This value was used to extrapolate the area from the last measured concentration to infinity.

**Cell Lines and Culture.** Human leukemic lymphoblasts (CCRF-CEM), a suspension line, were a gift of A. Fridland (St. Jude Children's Research Hospital, Memphis TN). Human colon carcinoma (HCT 116) and human colon adenocarcinoma (LoVo) cell lines were obtained from ATCC (Manassas, VA). These cell lines served as controls for calibration of immunosignals: CCRF-CEM for MGMT, HCT 116 for MSH-2 but not for MLH-1, and LoVo for MLH-1 but not for MSH-2. CCRF-CEM cells were grown in Eagle's MEM containing 10% newborn calf serum. HCT 116 were grown in McCoy's 5a medium containing 10% fetal bovine serum, and LoVo cells were grown in Ham's F-12 medium containing 20% fetal bovine serum.

**Extract Preparation.** Xenograft tissue was frozen in liquid nitrogen immediately after excision and ground under liquid nitrogen with mortar and pestle. The ground tissue was suspended in 3 volumes of extraction buffer (50 mM Tris-HCl, pH 7.5, 0.1 M NaCl, 2 mM EDTA, 1 mM DTT, containing protease inhibitors PMSF, aprotinin, benzamide, leupeptin, and pepstatin; Sigma Chemical Co., St. Louis, MO)

and homogenized three times for 10 s with a Brinkman Polytron homogenizer. The homogenate was sonicated three times for 10 s and centrifuged 30 min in a Beckman type 50 Ti rotor at 100,000  $\times$  g.

CCRF-CEM, HCT 116, and LoVo cell lines were each harvested, resuspended in 2 volumes of extraction buffer, and disrupted by three cycles of freeze thawing in liquid N<sub>2</sub>. Cell lysates were then centrifuged 14,000 rpm for 10 min in an Eppendorf microcentrifuge, and the supernatant was assayed for protein. All protein concentrations were determined according to the method of Bradford (23).

**Immunoblot Analysis.** Protein extracts (50  $\mu$ g) were separated by electrophoresis on Bio-Rad SDS denaturing Ready gels, 12% gels for MGMT analysis, and 7.5% gels for MLH-1 and MSH-2 analysis and then electroblotted to polyvinylidene difluoride membranes (Millipore, Bedford, MA) using 140 mA for 90 min in transfer buffer containing 25 mM Tris, 190 mM glycine, 15% methanol. Membranes were blocked with 5% nonfat dry milk in TBS-T (0.8% NaCl, 20 mM Tris-HCl, pH 7.6, and 0.1% Tween 20) and then allowed to air dry. Monoclonal antibody MT 3.1 (Chemicon, Temecula, CA) was biotinylated before use as primary antibody to probe the 12% gel blots for MGMT, followed by Streptavidin-biotinylated HRP complex (Amersham Pharmacia Biotech, Buckinghamshire England). Polyclonal antibodies MLH-1 (Ab-2) and MSH-2 (Ab-3; Calbiochem, La Jolla, CA) were used as primary antibodies to probe the 7.5% gel blots for MMR proteins, followed by anti-rabbit HRP-linked secondary antibody (from donkey; Amersham Pharmacia Biotech).  $\beta$ -tubulin was probed as a loading control using primary monoclonal antibody TUB 2.1 (Sigma) followed by antimouse HRP linked antibody (from sheep; Amersham Pharmacia Biotech). The enhanced chemiluminescence (ECL-Plus) system (Amersham Pharmacia Biotech) was used to develop the HRP signals on the membrane followed by brief exposure to X-ray film (Kodak X-Omat AR; Eastman Kodak Co., Rochester, NY). ECL generated signals were quantitated following densitometric scanning of fluorograms.

**p53-Isogenic Cell Lines.** NB1643 cells were transfected using calcium phosphate precipitation with either a control pcDNA3 plasmid or a pcDNA3 construct containing p53<sup>TDN</sup>. p53<sup>TDN</sup> is mutated at positions 14, 19, and 281 and exhibits a *trans*-dominant negative phenotype without the "gain of function" phenotype associated with some p53 mutants (24). Cells were selected using G418, and colonies were isolated and expanded. The colonies were then screened for overexpression of p53 and failure of  $\gamma$ -radiation (10 Gy, <sup>137</sup>Cs source) to induce a p21<sup>cip1</sup> response (see below). Two clones (p53<sup>TDN</sup>-1 and p53<sup>TDN</sup>-6) were used in the experiments reported. Clones were grown in RPMI 1640 containing 2 mM glutamine supplemented with 10% fetal bovine serum (Life Technologies) and 50 u/ml penicillin/50  $\mu$ g/ml streptomycin (Life Technologies) at 37°C with 5% CO<sub>2</sub>. For growth assays, cells were trypsinized in trypsin versene mixture (BioWhittaker) and plated at 2.5  $\times$  10<sup>5</sup> cells per 35-mm well in six-well plates (Costar, Corning NY). Triplicate wells of cells were treated with various concentrations of temozolomide. After 7 days, cells were harvested by trypsinization, and cell number was quantitated by nuclei counting. Data were plotted using Prism (GraphPad). Data are presented as mean  $\pm$  SE.

Table 1 Efficacy of temozolomide in neuroblastoma xenograft models

Tumor	Treatment (mg/kg)	No. in group	Average week tumor achieved 4× initial tumor volume (±1 SD)	Tumor growth delay (weeks)	Adjusted <i>P</i> <sup>a</sup>	No. of PRs	No. of CRs	MCR <sup>b</sup>	Time to reach nadir (weeks) <sup>c</sup>	Time to recover to initial tumor volume (weeks) <sup>d</sup>
NB-EB	Control	7	1.8 ± 0.8			0	0			
	66	7	7.8 ± 2.8	6.0	0.003	3	4	1	2	5
NB-1771	Control	6	2.8 ± 1.0			0	0			
	66	7	>12	>9.2	0.001	0	7	7	4	>12
NB-1382	Control	7	2.1 ± 0.4			0	0			
	66	7	>12	>9.9	0.001	0	7	7	2	>12
NB-1643	Control	7	3.2 ± 1.0			0	0			
	66	7	>12	>8.8	0.001	0	7	5	3	>12
NB-1691	Control	7	2.4 ± 1.0			0	0			
	66	6	2.8 ± 0.5	0.4	0.21	2	1	0	1	2
NB-1691	Control	7	4.7 ± 2.6			0	0			
	66	7	9.0 ± 1.7	4.3	0.005	5	0		2	6
NB-SD	Control	7	3.3 ± 1.4			0	0			
	66	7	>12	>8.7	0.001	3	1	1	9	11

<sup>a</sup> *P*s were obtained using exact log-rank tests (with Bonferroni correction procedure). *P*s compare tumor failure times among treatment groups and respective control group.

<sup>b</sup> Number of CRs maintained through week 12.

<sup>c</sup> Mean nadir for all tumors after start of treatment.

<sup>d</sup> Time for mean recovery to initial treatment volume.

**p21<sup>cip1</sup> Induction in NB1643 Cells.** NB1643pcDNA, p53<sup>TDN-1</sup>, or p53<sup>TDN-6</sup> were plated at either 2 or 4 × 10<sup>6</sup> cells/10-cm dish (Costar) and cultured for either 2 or 1 days, respectively, or at 1 × 10<sup>6</sup>/6-cm dish and cultured for 2 days. Cells were then treated with  $\gamma$  radiation (<sup>137</sup>Cs source), temozolomide, or doxorubicin at the doses indicated in the figures. Cells were then lysed 24 h later in 400  $\mu$ l (10-cm dishes) or 100  $\mu$ l (6-cm dishes) of SDS-PAGE sample buffer preheated to 100°C. Lysates were repipetted four times through a 25 G needle. Forty  $\mu$ l of each sample were loaded for resolution using SDS-PAGE. The gels were transferred to Immobilon-P (Millipore) using the *Trans*-Blot electrophoretic transfer cell (Bio-Rad) containing Tris/glycine/methanol transfer buffer [25 mM Tris, 192 mM glycine, pH 8.3, and 20% (v/v) methanol] under a constant voltage of 100 V for 1 h. Membranes were blocked for 1 h in 5% milk in TBST (10 mM Tris-HCl, pH 8.0, 150 mM NaCl, 0.05% Tween-20) at 22°C. Blots were washed once for 15 min and twice for 5 min with TBST and then incubated with anti-p21<sup>cip1</sup> antibodies (Santa Cruz) in 1% milk/1% BSA in TBST for 1 h. The membranes were then washed as above and incubated with antirabbit or antimouse horseradish peroxidase in 1% milk/1% BSA in TBST for 1 h. The membranes were then washed for 15 min and then four times more for 5 min in TBST. Protein bands were then visualized using chemiluminescent detection with the ECL (Amersham Pharmacia Biotech) and XAR 5 film (Kodak).

## RESULTS

**Control of Tumor Growth.** The purpose of this study was to relate the sensitivity of a series of human tumors in mice to certain phenotypic characteristics of these xenografts (MGMT, MMR, and p53), with a goal subsequently to conduct a similar study relating the tumor phenotype to responsiveness in a clinical trial of temozolomide. For this preclinical study, therefore, we have used a schedule of drug administration that

parallels that used clinically, drug dose levels that in mice approximate systemic exposures that are achieved in patients, and tumor response criteria that relate to those used to define tumor response in patients. Tumors have been classified as having high, intermediate, or low sensitivity based on the response criteria given in "Materials and Methods." Mice received temozolomide by oral gavage daily for 5-days. Cycles of treatment were repeated every 21 days over 8 weeks. The MTD for three cycles of treatment was 66 mg/kg per administration (200 mg/m<sup>2</sup>) on this schedule. Higher dose levels (100 mg/kg/dose) caused deaths during the second cycle of therapy (data not presented). Tables 1–3 show the results of the exact log-rank tests used to compare differences in the distributions of tumor failure times among temozolomide treatment groups compared to control groups for neuroblastoma, rhabdomyosarcoma, and brain tumors, respectively.

As shown in Tables 1–3, temozolomide induced CR that was maintained at week 12 in all mice bearing NB-1382, NB-1771 neuroblastomas, Rh30 and Rh30c rhabdomyosarcoma, and SJ-BT27 medulloblastoma. These tumors were classified as having high sensitivity to treatment with this agent. At least PRs were obtained against Rh28 and neuroblastomas NB-EB and NB-1643. In one experiment, all D283 medulloblastomas demonstrated  $\geq$ PR, but in other experiments, although temozolomide significantly inhibited growth, few PRs were obtained (Table 3). Approximately half of all of the tumors examined were classified as having low sensitivity to temozolomide. In these tumor lines there were relatively few PRs, although significant tumor growth inhibition was observed for some lines (notably NB-SD, Rh12, and GBM2; Tables 1–3). The time for tumors in a treatment group to regress to the group nadir, and duration of regression is also presented for each tumor (Tables 1–3). Overall, temozolomide induced objective regressions (>50% decrease in volume) in 8 of 17 tumor lines examined at the MTD on this daily times 5 schedule.

Table 2 Efficacy of temozolomide in rhabdomyosarcoma xenograft models

Tumor	Treatment	No. in group	Average week tumor achieved 4× initial tumor volume (1 SD)	Tumor growth delay (weeks)	Adjusted $P^a$	No. of PRs	No. of CRs	MCR <sup>b</sup>	Time to reach nadir (weeks) <sup>c</sup>	Time to recover to initial tumor volume (weeks) <sup>d</sup>
Rh12 <sup>c</sup>	Control	4	2.3 ± 0.5			0	0			
	66	6	9	6.7	0.005	0	1	0	1	2
Rh12 <sup>c</sup>	Control	5	4 ± 1.2			0	0			
	66	7	6	2	0.005	0	0		2	3
Rh18 <sup>c</sup>	Control	7	3.3 ± 0.8			0	0			
	66	6	6 ± 2.1	2.7	0.070	2	0		1	2
Rh18 <sup>c</sup>	Control	6	3.4 (0.5)			0	0			
	66	7	(9.3 ± 3.1)	5.9	0.008	3	1	0	2	3
Rh28	Control	6	3.7 ± 1.2			0	0			
	66	7	10	6.3	0.001	6	1	0	4	8
Rh28 <sup>c</sup>	Control	5	3.2 ± 0.4			0	0			
	66	7	9.8 ± 2.2	6.6	0.023	2	0		NR <sup>d</sup>	NR
Rh30	Control	4	4.3 ± 1.0			0	0			
	66	7	>12	>7.7	0.003	0	7	7	3	>12
Rh66	Control	7	4.1 ± 1.1			0	0			
	66	7	10 ± 1	5.9		2	1	0	2	8

<sup>a</sup>  $P$ s were obtained using exact log-rank tests (with Bonferroni correction procedure).  $P$ s compare tumor failure times among treatment groups and respective control group.

<sup>b</sup> Number of CRs maintained through week 12.

<sup>c</sup> Replicate studies.

<sup>d</sup> NR, no regression.

Table 3 Efficacy of temozolomide in brain tumor xenograft models

Tumor	Treatment	No. in group	Average week tumor achieved 4× initial tumor volume (1 SD)	Tumor growth delay (weeks)	Adjusted $P^a$	No. of PRs	No. of CRs	MCR <sup>b</sup>	Time to reach nadir (weeks) <sup>c</sup>	Time to recover to initial tumor volume (weeks) <sup>d</sup>
D283	Control	5	5.3 ± 0.5			0	0			
	66	7	>12	>6.7	0.001	3	4	0	3	9
D283 <sup>c</sup>	Control	6	2.6 ± 0.9			0	0			
	66	7	6.8 ± 0.4	4.2	0.004	2	0		1	2
D283 <sup>c</sup>	Control	5	4 ± 1			0	0			
	66	7	8.4 ± 1.5	4.4	0.005	3	0		2	5
SJ-BT27	Control	6	3 ± 1.1			0	0	0		
	66	7	>12	>9	0.001	0	7	7	2	>12
SJ-BT29	Control	6	3.6 ± 0.5			0	0			
	66	4	6.4 ± 1.8	2.8	0.02	0	0	0	NR <sup>d</sup>	NR
SJ-GBM2	Control	7	2.4 ± 0.5			0	0			
	66	7	8.7 ± 0.6	5.3	0.002	0	2	0	4	5
SJ-GBM2 <sup>c</sup>	Control	7	3.5 ± 1			0	0			
	66	7	10.5 ± 2.1	7	0.001	3	1	0	4	9

<sup>a</sup>  $P$ s were obtained using exact log-rank tests (with Bonferroni correction procedure).  $P$ s compare tumor failure times among treatment groups and respective control group.

<sup>b</sup> Number of CRs maintained through week 12.

<sup>c</sup> Replicate studies.

<sup>d</sup> NR, no regression.

**Pharmacokinetics.** To determine whether temozolomide plasma systemic exposure was relevant to responses of human cancer at the dose level administered, we determined the plasma levels of temozolomide and MTIC. Temozolomide and MTIC concentrations exceeded the limit of assay sensitivity for the duration of the study. Following oral administration (66 mg/kg), the apparent  $t_{\max}$  was 15 min for temozolomide and 30 min for MTIC. The  $C_{\max}$  values for temozolomide and MTIC were 20 and 0.8 mg/ml respectively. The plasma  $AUC_{0 \rightarrow \infty}$  for temozolomide and MTIC were 40 and 1.9 mg/l-h, respectively.

**DNA Repair Phenotypes.** Tumor sensitivity to temozolomide administered at the MTD on the daily times 5 schedule is related to the tumor phenotype in Table 4. The primary repair mechanism for resistance to temozolomide is MGMT. We therefore determined the MGMT levels in (untreated) tumor extracts from the xenograft lines that had been characterized for temozolomide response. Immunoblots shown in Fig. 2 indicate that MGMT varies from relatively high levels to complete suppression. The amounts of MGMT protein were quantitated by densitometry relative to CEM cells and ranked as described in Table

Table 4 Relationship between sensitivity of xenografts to temozolomide and DNA repair or p53 phenotype

Tumor line	MGMT status <sup>a</sup>	MSH2 status <sup>b</sup>	MLH1 status <sup>c</sup>	p53 status <sup>d</sup>
High sensitivity				
Rh30	—	++	±	mt/wt
Rh30c	—	+	+	mt/wt
BT-27	—	++	±	?
NB-1771	+	++	++	?
NB-1382	±	++	++	wt
Intermediate sensitivity				
NB-1643	—	+	+	wt/functional
NB-EB	±	++	+	wt/functional
Rh28	—	++	—	wt
[D283]	+	++	+	mt
Low sensitivity				
[D283]	+	++	+	mt
Rh18	++	±	—	wt/MDM2 amp
Rh66	++	++	+	?
Rh12	++	++	+	wt
BT-29	++	++	+	?
NB-1691	++	—	—	wt/MDM2 amp
NB-SD	±	++	±	mt
GBM2	—	++	±	mt
Rh28c	—	++	—	wt/nonfunctional

<sup>a</sup> MGMT relative to CEM cell level: —, <0.05; +, 0.05–0.5; ++, >0.5.

<sup>b</sup> MLH-1 relative to LoVo cell level: —, <0.05; +, 0.05–0.5; ++, >0.5.

<sup>c</sup> MSH-2 relative to HCT116 cell level: —, <0.5; +, 0.5–1.0; ++, >1.0.

<sup>d</sup> wt, wild type; mt, mutant; amp, amplified; ?, not determined.

4. How MGMT protein levels relate to the tumor responses to temozolomide is shown in Table 4. Generally, the most responsive tumors (four of five) are totally deficient or have very low MGMT. In contrast, among the most resistant tumors, five of nine had high levels of MGMT. Responses of two rhabdomyosarcoma lines that differ primarily in their MGMT levels (their MMR proteins being similar) are shown in Fig. 3, A, B, C, and D. Temozolomide, even at the highest tolerated dose level (66 mg/kg), failed to cause appreciable regressions in Rh12 tumors with high level MGMT, whereas MGMT-deficient Rh30c tumors treated with only 28 mg/kg temozolomide regressed completely with no regrowth.

The role of MMR was assessed by similar quantitation of the MMR proteins MLH-1 and MSH-2. Immunoblot data are shown in Fig. 2, and the values relative to control cells LoVo (MLH-1) and HCT116 (MSH-2) are indicated in Table 4. Except for SJ-BT27 and Rh30, which have low MLH-1 levels, the MMR proteins appear to be present in significant amounts in all of the sensitive tumors, as would be expected.

Among nine resistant (and three intermediate sensitivity) tumors, four are completely deficient and two have only marginal levels of at least one of the MMR proteins. Most significantly, those tumors in this group that are deficient in MGMT (Rh28/Rh28c and GBM2) and that, based on this criterion alone, we would predict to be drug sensitive, are also compromised by impaired MMR. Responses of rhabdomyosarcomas Rh30c and Rh28c, which differ notably in their levels of MLH-1, are shown in Fig. 3, A, B, E and F. Both lack MGMT; however, MLH-1-competent Rh30c tumors were highly sensitive to temozolomide at a dose of 28 mg/kg, whereas MLH-1 deficient Rh28c xenografts were highly refractory to treatment at the MTD of 66 mg/kg.

**Role of p53 in Temozolomide Sensitivity.** Temozolomide-induced apoptosis may be dependent or independent of p53 function (12), although p53 may sensitize cells to this agent (8). Because there is a report that temozolomide may induce p53 protein (13), we tested the role that p53 has in temozolomide sensitivity using paired neuroblastoma cell lines differing in functional p53 status. NB1643 cells were engineered to overexpress a TDN p53 protein. This TDN p53 protein, which has mutations at positions 14, 19, and 281, does not exhibit the gain of function phenotype that is associated with some mutations in p53.  $\gamma$ -Radiation induces p21<sup>cip1</sup> expression in NB1643pcDNA3, whereas  $\gamma$ -radiation does not induce p21<sup>cip1</sup> expression in either NB1643p53<sup>TDN-1</sup> or p53<sup>TDN-6</sup> (Fig. 4A). We conclude that NB1643pcDNA retains wild type functional p53, whereas the resulting cell clones, NB1643p53<sup>TDN-1</sup> and NB1643p53<sup>TDN-6</sup>, do not have functional p53 status. Growth inhibition assays were performed with temozolomide using these paired cell lines; temozolomide has similar activity against both the parental line with functional p53 and NB1643p53<sup>TDN-1</sup> (Fig. 4B). Unexpectedly, one of the nonfunctional p53 lines, NB1643p53<sup>TDN-6</sup>, is more sensitive to temozolomide. Further characterization showed that MGMT was undetectable in NB1643p53<sup>TDN-6</sup>, whereas both the NB1643p53pcDNA3 and NB1643p53<sup>TDN-1</sup> clones expressed MGMT, albeit at very low levels (Table 5). Both of the MMR proteins were present at appreciable levels in all three clones. Therefore, it seems likely that the differing drug sensitivities of these lines do not involve functional p53 but rather other proteins involved in determining drug sensitivity to temozolomide, such as MGMT. We next tested whether temozolomide induces p21<sup>cip1</sup> in these paired neuroblastoma clones. In contrast to  $\gamma$ -radiation (5 Gy), temozolomide did not induce p21<sup>cip1</sup> in either parental or p53<sup>TDN-1</sup>

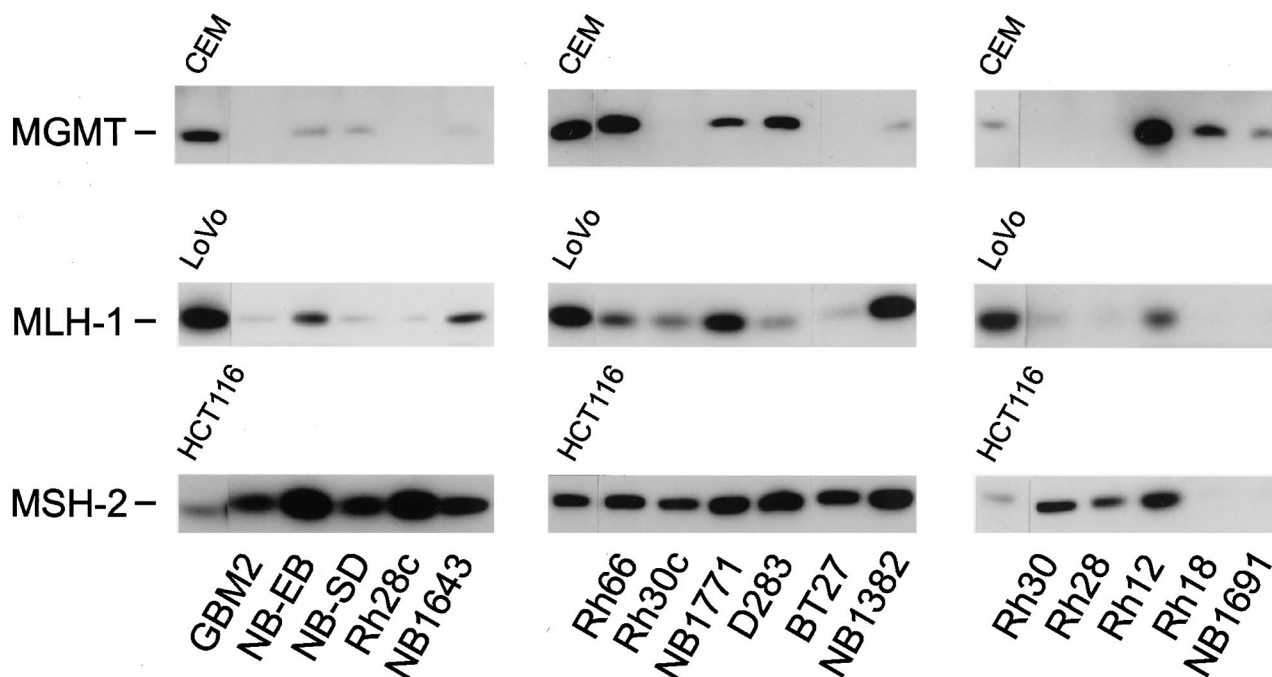


Fig. 2 Western analysis of MGMT, MLH-1, and MSH-2 in human tumor xenografts. Fifty  $\mu$ g of extract protein were loaded on each lane. Standard cell extracts (50  $\mu$ g) were included in each blot; CEM for MGMT, LoVo for MLH-1, and HCT116 for MSH-2. Each protein was probed with the appropriate antibody on separate blots as described in "Materials and Methods." Each blot was also probed anti- $\beta$ -tubulin to ensure equivalent loading (data not shown).

cells 4 h after exposure (Fig. 4C). To determine whether there was a delayed response to temozolomide (that required at least one cell cycle time), NB1643pcDNA3 cells were exposed to temozolomide or the topoisomerase II poison doxorubicin for up to 72 h (Fig. 4D). Doxorubicin induces p21<sup>cip1</sup> in the vector control cells. Exposure for up to 72 h to temozolomide (100–200  $\mu$ M) did not induce p21<sup>cip1</sup> in NB1643pcDNA3 cells.

## DISCUSSION

The activity of temozolomide as a single agent was examined against 15 independently derived xenografts and two additional sublines. The highest dose tolerated for three cycles of treatment using the daily times five schedule was 66 mg/kg (approximately 200 mg/m<sup>2</sup>, similar to the dose used clinically for pediatric patients not previously treated with craniospinal radiation). At this dosage, CR was measured in four tumor lines and one subline. Interestingly, two tumors (NB-1382 and SJ-BT27) were exquisitely sensitive, demonstrating CRs at 14 and 9.5 mg/kg/day (data not shown). Temozolomide also induced PR in three tumor lines (NB-EB, NB-1643, and Rh28). Stable disease or slowed progression was measured in the other tumors (eight lines and one subline). Thus, against this panel of pediatric solid tumors temozolomide, administered by oral gavage at the MTD induced an objective responses rate of 47%.

The results of our pharmacokinetic studies show that the temozolomide AUC was similar to that reported by other investigators in both rodents and patients. Gallo and colleagues (25) administered temozolomide intraarterially at a dose of 40 mg/kg in the glioma-bearing rat model and reported a temozolomide

AUC of 17.3 mg/l-h. In addition, Stevens *et al.* (26) administered temozolomide p.o. to mice (20 mg/kg), and based upon interpolation of data presented in a figure, the temozolomide AUC was approximately 38 mg/l-h. Data from patients receiving temozolomide 100 mg/m<sup>2</sup> showed an AUC of 16 mg/l-h (27), which is consistent with the results presented in the present study. Moreover, Reid *et al.* (21) administered a dose of 200 mg/m<sup>2</sup> and reported a temozolomide AUC of approximately 30 mg/l-h. However, the MTIC values reported by Baker *et al.* (27) and Reid *et al.* (Ref. 21; 0.628 and 0.636 mg/l-h) are somewhat lower than levels observed in our xenograft model.

Sensitivity of each tumor to temozolomide was next compared to the expression of MGMT and MMR proteins MSH-2 and MLH-1. Each tumor classified as highly sensitive or of intermediate sensitivity has low levels of MGMT. Of note is that MGMT could not be detected by immunoblot analysis in one neuroblastomas (NB-1643), two rhabdomyosarcomas and their sublines (Rh28, Rh28c, and Rh30, Rh30c), one medulloblastoma (SJ-BT27), and the glioma (SJ-GBM2). Each of the tumors having high or intermediate sensitivity demonstrated detectable MSH-2 and MLH-1 proteins. Tumors classified as having low sensitivity appear to fall into two groups: those with high MGMT and detectable expression of MSH-2 and MLH-1 and those with a wide range of MGMT (Rh12, Rh66, D283, and SJ-BT29) but with undetectable or marginal MLH-1 (Rh18, Rh28c, NB-SD, NB-1691, and SJ-GBM2). The contribution of MGMT to intrinsic resistance is best judged from comparison of responses in sensitive tumors, such as Rh30c (Fig. 3, A and B), and NB-1643 versus insensitive tumors, such as Rh12 (Fig. 3, C

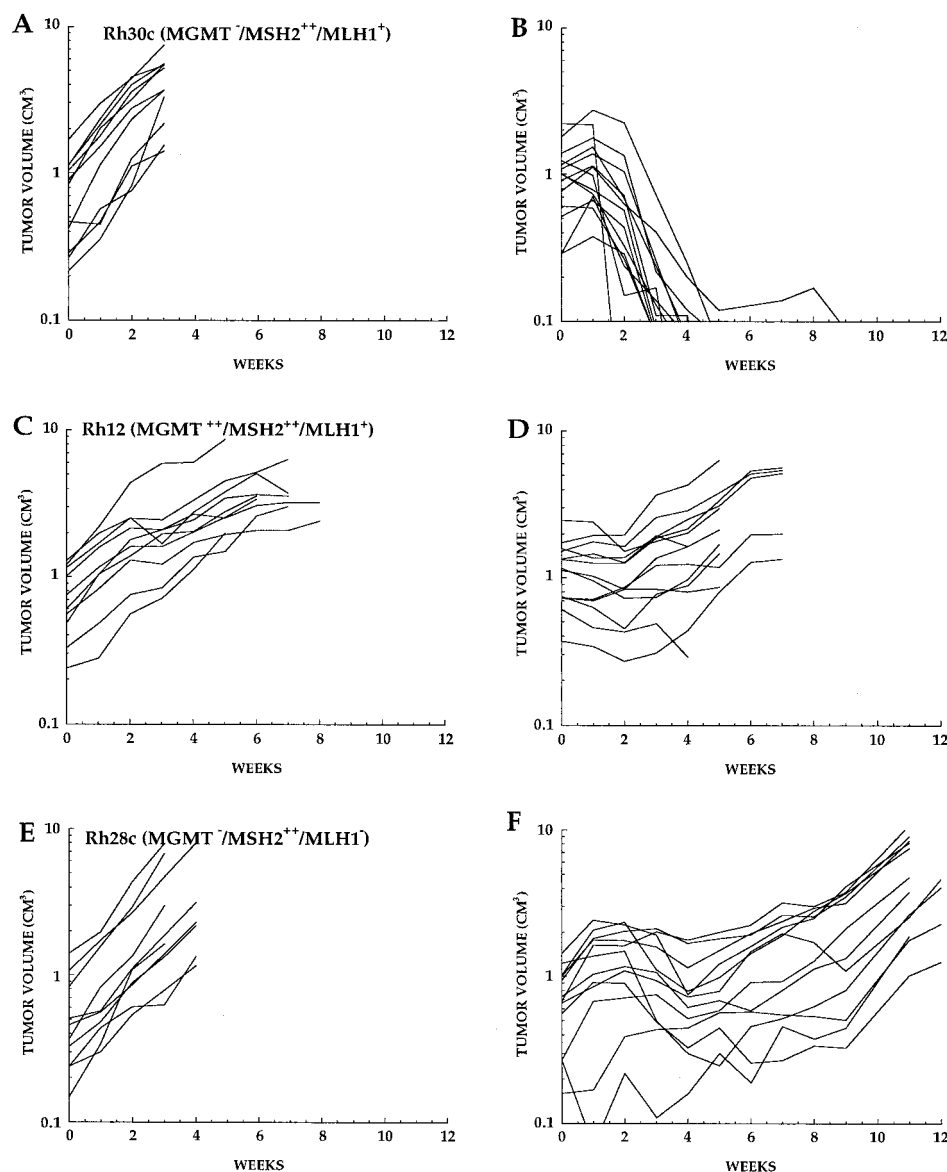


**Fig. 3** Sensitivity of rhabdomyosarcoma xenografts to temozolomide treatment. *Left panels*, growth of control tumors. Temozolomide was administered by oral gavage daily for 5 days at 28 mg/kg (*B*, Rh30c) or 66 mg/kg (*D* and *E*, Rh12 and Rh28c, respectively). Courses of treatment were repeated every 21 days for three cycles. Each *curve* represents the growth of an individual tumor

and *D*) and Rh66, that all have similar expression of MLH-1 and MSH-2 but differ only in expression of MGMT. Similarly, MGMT status appears to be the major difference between two medulloblastomas, SJ-BT27 and SJ-BT29. The importance of MMR can be estimated by comparison of sensitive tumors that are MGMT negative but MMR competent (Rh30c, NB-1643, and NB-EB) with tumors that are MGMT negative but also MLH-1 negative [Rh28c (Fig. 3, *E* and *F*) and SJ-GBM2]. These tumors responded poorly to temozolomide, although treatment caused significant growth inhibition. Our results suggest that high levels of MGMT predict intrinsic resistance to temozolomide in agreement with other reports. However, for tumors with low or undetectable MGMT, MMR-status is an important determinant of response. These results are in general consistent with the mechanisms shown in Fig. 1. However it should be pointed out that other factors, such as methylation adducts other

than *O*<sup>6</sup>-methylguanine in DNA, and other cellular resistance mechanisms or extracellular factors, such as drug distribution, may also play a role in the responses to temozolomide therapy.

The importance of p53 function is less readily defined from these studies. Temozolomide did not induce p53 or p21<sup>cip1</sup> expression in NB1643 cells at a concentration of drug that inhibited growth by >90%. *In vitro*, suppression of p53 function in NB-1643 clones, engineered to express a *trans*-dominant p53, did not lead to temozolomide resistance. Rather, one clone was more sensitive possibly due to decreased MGMT, and one clone that was slightly more resistant, expressed slightly higher MGMT than the vector control clone. It should be noted that MGMT levels in all of these clones were extremely low in comparison to CCRF-CEM leukemic cells used as the standard for MGMT expression. Although these NB-1643 clones are derived from a common parental cell line, a loss of p53 may

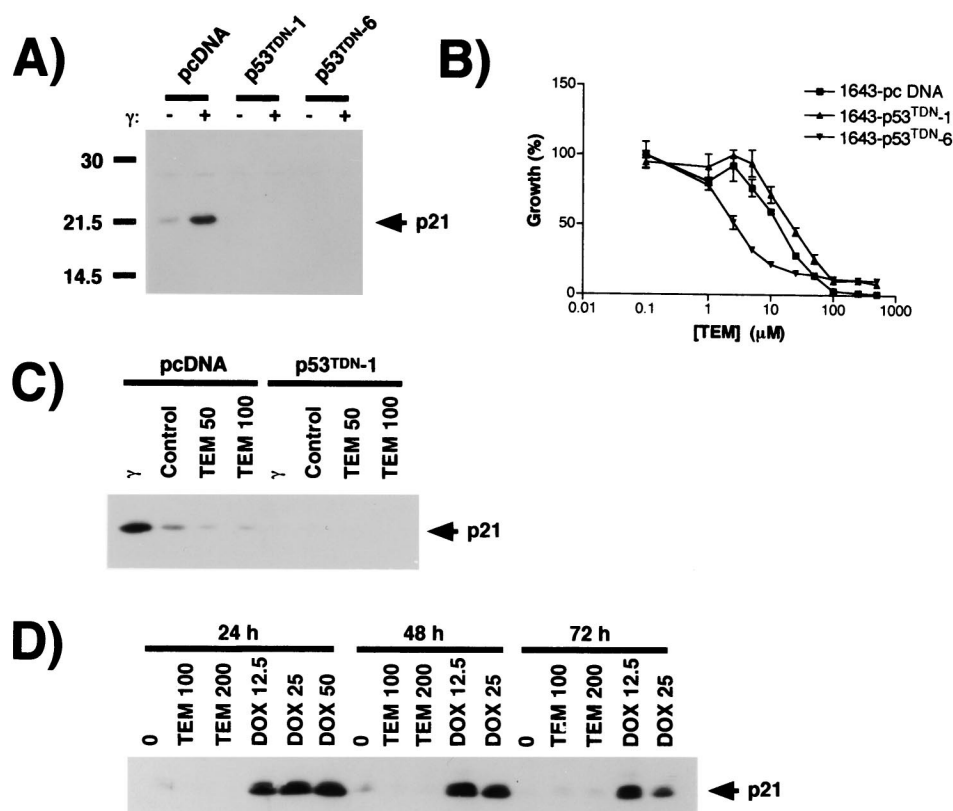


**Fig. 4** Temozolomide sensitivity is not dependent on functional p53 in NB1643 cells. **A**, p21<sup>cip1</sup> protein induction after ionizing radiation (5 Gy). NB1643pcDNA3 cells, NB1643p53<sup>TDN-1</sup> and -6 clones expressing the TDN p53 were irradiated and p21<sup>cip1</sup> expression determined after 4 h by immunoblotting. **B**, growth inhibition of NB1643pcDNA3, p53<sup>TDN-1</sup>, and p53<sup>TDN-6</sup> by temozolomide (*TEM*) is not dependent on functional p53 status. NB1643 pcDNA, p53<sup>TDN-1</sup>, or p53<sup>TDN-6</sup> cells were plated in complete medium, then treated with temozolomide 24 h later and cultured for 7 days. Cell number was determined by nuclei counting. **C**, temozolomide treatment does not induce p21<sup>cip1</sup> expression in NB1643 pcDNA or p53<sup>TDN-1</sup> cells. Cells were treated with  $\gamma$  radiation (5 Gy) or 50 or 100  $\mu$ M temozolomide, lysed after 4 h, and then immunoblotted to detect p21<sup>cip1</sup> expression. **D**, temozolomide does not induce p21<sup>cip1</sup> expression in NB1643 cells, whereas doxorubicin does induce p21<sup>cip1</sup> expression in these cells. NB1643pcDNA3 cells were treated with either 100 or 200  $\mu$ M temozolomide or 12.5, 25, or 50 nM doxorubicin. Cells were lysed at 24, 48, and 72 h after drug treatment and immunoblotted to detect p21<sup>cip1</sup> expression. The concentrations of doxorubicin and temozolomide used are estimated to result in greater than 90% growth inhibition in 7 days.

**Table 5** Relative levels of DNA repair proteins in NB1643 clones transfected with control plasmid or a trans-dominant negative p53 construct

Clone	MGMT clone/CEM	MLH-1 clone/LoVo	MSH-2 clone/HCT16
pcDNA3	0.01	1.15	2.36
p53 <sup>TDN-1</sup>	0.17	0.62	2.5
p53 <sup>TDN-6</sup>	ND <sup>a</sup>	0.62	2.05

<sup>a</sup> Not detectable.

facilitate rapid accumulation of other changes. Hence, it is quite possible that the differences in temozolomide sensitivity of these clones are due to damage or resistance factors unrelated to MGMT or MMR.

The notion that p53 is required for MMR-induced apoptosis is not supported by data from the NB1643 model. Although p53 may be induced by MMR processing of temozolomide damage, there probably are other redundant pathways for apoptosis.

In summary, at therapeutically relevant systemic expo-

sure, temozolomide demonstrates significant activity against a panel of childhood solid tumors heterografted in immune-deprived mice. The dose level used achieves plasma levels of MTIC consistent with plasma systemic exposures that are reported in children using 200 mg/m<sup>2</sup>. These results suggest temozolomide may have activity in childhood neoplasms other than brain tumors.

The major mechanism for temozolomide resistance *in vivo* appears to be MGMT; however, potentially responsive MGMT-deficient tumors may escape by virtue of defective MMR. Consequently, based on the data presented, it should be possible to predict therapeutic outcome and guide the clinical use of this drug in combination with an MGMT inhibitor such as *O*<sup>6</sup>-benzylguanine. However, further studies to determine MMR and MGMT status of patient tumors will be necessary to validate the predictions based on the xenografts used in this study.

#### ACKNOWLEDGMENTS

We thank Joanna Remack, Pamela Cheshire, and Lois Richmond for excellent technical assistance.

## REFERENCES

- Bleehen, N. M., Newlands, E. S., Lee, S. M., Thatcher, N., Selby, P., Calvert, A. H., Rustin, G. J., Brampton, M., Stevens, M. F. Cancer Research Campaign Phase II trial of temozolomide in metastatic melanoma. *J. Clin. Oncol.*, 13: 910–913, 1995.
- Bower, M., Newlands, E. S., Bleehen, N. M., Bada, M., Begent, R. J., Calvert, A. H., Colquhoun, I., Lewis, P., Brampton, M. H. Multicentre CRC Phase II trial of temozolomide in recurrent or progressive high-grade glioma. *Cancer Chemother. Pharmacol.*, 40: 484–488, 1997.
- Newlands, E. S., Stevens, M. F. G., Wedge, S. R., Wheelhouse, R. T., Brock, T. M. Temozolomide: a review of its discovery, chemical properties, pre-clinical development and clinical trials. *Cancer Treat. Rev.*, 23: 35–61, 1997.
- Tisdale, M. J. Antitumor imidazotetrazine. XV. Role of guanine  $O^6$  alkylation in the mechanism of cytotoxicity of imidazotetrazines. *Biochem. Pharmacol.*, 36: 457–462, 1987.
- Wedge, S. R., Porteus, J. K., May, B. L., and Newlands, E. S. Potentiation of temozolomide and BCNU cytotoxicity by  $O(6)$ -benzylguanine: a comparative study *in vitro*. *Br. J. Cancer*, 73: 482–490, 1996.
- Graziani, G., Faraoni, I., Grohmann, U., Bianchi, R., Binaglia, L., Margison, G. P., Watson, A. J., Orlando, L., Bonmassar, E., and D'Atri, S.  $O^6$ -alkylguanine-DNA alkyltransferase attenuates triazene-induced cytotoxicity and tumor cell immunogenicity in murine L1210 leukemia. *Cancer Res.*, 55: 6231–6236, 1995.
- Branch, P., Aquilina, G., Bignami, M., and Karran, P. Defective mismatch binding and a mutator phenotype in cells tolerant to DNA damage. *Nature (Lond.)*, 362: 652–654, 1993.
- Tentori, L., Lecal, P. M., Benincasa, E., Franco, D., Faraoni, I., Bonmassar, E., and Graziani, G. Role of wild-type p53 on the antineoplastic activity of temozolomide alone or combined with inhibitors of poly(ADP-ribose) polymerase. *J. Pharmacol. Exp. Ther.*, 285: 884–893, 1998.
- Kolodner, R. Biochemistry and genetics of eukaryotic mismatch repair. *Genes Dev.*, 10: 1433–1442, 1996.
- Thibodeau, S. N., French, A. J., Roche, P. C., Cunningham, J. M., Tester, D. J., Lindor, N. M., Moslein, G., Baker, S. M., Liskay, R. M., Burgart, L. J., Honchel, R., and Halling, K. C. Altered expression of hMSH2 and hMLH1 in tumors with microsatellite instability and genetic alterations in mismatch repair genes. *Cancer Res.*, 56: 4836–4840, 1996.
- Liu, L., Markowitz, S., and Gerson, S. L. Mismatch repair mutations override alkyltransferase in conferring resistance to temozolomide but not to 1,3-bis(2-chloroethyl)nitrosourea. *Cancer Res.*, 56: 5375–5379, 1996.
- Tentori, L., Orlando, L., Lecal, P. M., Benincasa, E., Faraoni, I., Bonmassar, E., D'Atri, S., and Graziani, G. Inhibition of  $O^6$ -alkylguanine DNA-alkyltransferase or poly(ADP-ribose) polymerase increases susceptibility of leukemic cells to apoptosis induced by temozolomide. *Mol. Pharmacol.*, 52: 249–258, 1997.
- D'Atri, S., Tentori, L., Lecal, P. M., Graziani, G., Pagani, E., Benincasa, E., Zambruno, G., Bonmassar, E., and Jiricny, J. Involvement of the mismatch repair system in temozolomide-induced apoptosis. *Mol. Pharmacol.*, 54: 334–341, 1998.
- Houghton, P. J., Cheshire, P. J., Hallman, J. D., Lutz, L., Friedman, H. S., Danks, M. K., and Houghton, J. A. Efficacy of topoisomerase I inhibitors, topotecan and irinotecan, administered at low dose levels in protracted schedules to mice bearing xenografts of human tumors. *Cancer Chemother. Pharmacol.*, 36: 393–403, 1995.
- Houghton, P. J., Cheshire, P. J., Hallman, J. C., Bissery, M. C., Mathieu-Boue, A., and Houghton, J. A. Therapeutic efficacy of the topoisomerase I inhibitor 7-ethyl-10(4-[1-piperidino]-1-piperidino)-carboxyloxy-camptothecin against human tumor xenografts: Lack of cross-resistance *in vivo* in tumors with acquired resistance to the topoisomerase I inhibitor 9-dimethylaminomethyl-10-hydroxycamptothecin. *Cancer Res.*, 53: 2823–2829, 1993.
- Thompson, J., Zamboni, W. C., Cheshire, P. J., Lutz, L., Luo, X., Li, Y., Houghton, J. A., Stewart, C. F., and Houghton, P. J. Efficacy of systemic administration of irinotecan against neuroblastoma xenografts. *Clin Cancer Res.*, 3: 423–431, 1997.
- Zamboni, W. C., Stewart, C. F., Thompson, J., Santana, V., Cheshire, P. J., Richmond, L. B., Liu, X., Houghton, J. A., and Houghton, P. J. The relationship between topotecan systemic exposure and tumor response in human neuroblastoma xenografts. *J. Natl Cancer Inst.*, 90: 505–511, 1998.
- Hochberg, Y., and Tamhane, A. Multiple Comparison Procedures, pp. 94–96. New York: John Wiley & Sons, 1987.
- Shen, F., Decosterd, L. A., Gander, M., Leyvraz, S., Biollaz, J., and Lejeune, F. Determination of temozolomide in human plasma and urine by high-performance liquid chromatography after solid-phase extraction. *J. Liquid Chromatogr. B*, 667: 291–300, 1995.
- Newlands, E. S., Blackledge, G. R. P., Slack, J. A., Rustin, G. J. S., Smith, D. B., Stuart, N. S. A., Quarterman, C. P., Hofman, R., Stevens, M. F. G., Brampton, M. H., and Gibson, A. C. Phase I trial of temozolomide (CCRG 81045; M&B 39831; NSC 362856). *Br. J. Cancer*, 65: 287–291, 1992.
- Reid, J. M., Stevens, D. C., Rubin, J., and Ames, M. M. Pharmacokinetics of 3-methyl-(triazene-1-yl)imidazole-4-carboximide following the administration of temozolomide to patients with advanced cancer. *Clinical Cancer Res.*, 3: 2393–2398, 1997.
- Yeh, K. C., and Kwan, K. C. A comparison of numerical integrating algorithms by trapezoidal, Lagrange, and spline approximation. *J. Pharmacokin. Biopharm.*, 6: 79–98, 1978.
- Bradford, M. M. A rapid and sensitive method for the quantitation of microgram quantities of protein using the principle of protein-dye binding. *Anal. Biochem.*, 72: 248–254, 1976.
- Thottassery, J. V., Zambetti, G. P., Arimori, K., Schuetz, E. G., and Schuetz, J. D. p53-dependent regulation of MDR1 gene expression causes selective resistance to chemotherapeutic agents. *Proc. Natl. Acad. Sci. USA*, 94: 11037–11042, 1997.
- Devineni, D., Klein-Szanto, A., and Gallo, J. M. Uptake of temozolomide in a rat glioma model in the presence and absence of the angiogenesis inhibitor TNP-470. *Cancer Res.*, 56: 1983–1987, 1996.
- Stevens, M. F. G., Hickman, J. A., Langdon, S. P., Chubb, D., Vickers, L., Stone, R., Baig, G., Goddard, C., Gibson, N. W., Slack, J. A., Newton, C., Lunt, E., Fizames, C., and Lavelle, F. Antitumor activity and pharmacokinetics in mice of 8-carbamoyl-3-methylimidazo[5,1-d]-1,2,3,5-tetrazin-4(3H)-one (CCRG 81045; M & B 3981), a novel drug with potential as an alternative to dacarbazine. *Cancer Res.*, 47: 5846–5852, 1987.
- Baker, S. D., Wirth, M., Statkevich, P., Reidenberg, P., Alton, K., Sartorius, S. E., Dugan, M., Cutler, D., Batra, V., Grochow, L. B., Donehower, R. C., and Rowinsky, E. K. Absorption, metabolism, and excretion of  $^{14}$ C-temozolomide following oral administration to patients with advanced cancer. *Clinical Cancer Res.*, 5: 309–317, 1999.

# Clinical Cancer Research

## Biochemical Correlates of Temozolomide Sensitivity in Pediatric Solid Tumor Xenograft Models

David S. Middlemas, Clinton F. Stewart, Mark N Kirstein, et al.

*Clin Cancer Res* 2000;6:998-1007.

**Updated version** Access the most recent version of this article at:  
<http://clincancerres.aacrjournals.org/content/6/3/998>

**Cited articles** This article cites 21 articles, 13 of which you can access for free at:  
<http://clincancerres.aacrjournals.org/content/6/3/998.full#ref-list-1>

**Citing articles** This article has been cited by 30 HighWire-hosted articles. Access the articles at:  
<http://clincancerres.aacrjournals.org/content/6/3/998.full#related-urls>

**E-mail alerts** [Sign up to receive free email-alerts](#) related to this article or journal.

**Reprints and Subscriptions** To order reprints of this article or to subscribe to the journal, contact the AACR Publications Department at [pubs@aacr.org](mailto:pubs@aacr.org).

**Permissions** To request permission to re-use all or part of this article, use this link  
<http://clincancerres.aacrjournals.org/content/6/3/998>.  
Click on "Request Permissions" which will take you to the Copyright Clearance Center's (CCC) Rightslink site.